

Refereed Proceedings

*The 12th International Conference on
Fluidization - New Horizons in Fluidization
Engineering*

Engineering Conferences International

Year 2007

Numerical Study of the Intrinsic and
Feedback Dynamics of a Gas-Solid
Fluidized Bed

F. Bonniol* C. Sierra† R. Occelli‡
H. Bournot** L. Tadriss††

*Laboratoire de l'IUSTI, Polytech' Marseille – DME, florian.bonniol@polytech.univ-mrs.fr

†Laboratoire de l'IUSTI, Polytech' Marseille – DME, christophe.sierra@polytech.univ-mrs.fr

‡Laboratoire de l'IUSTI, Polytech' Marseille – DME, rene@polytech.univ-mrs.fr

**Laboratoire de l'IUSTI, Polytech' Marseille – DME, herve.bournot@polytech.univ-mrs.fr

††Laboratoire de l'IUSTI, Polytech' Marseille – DME, lounes.tadriss@polytech.univ-mrs.fr

This paper is posted at ECI Digital Archives.

http://dc.engconfintl.org/fluidization_xii/79

Bonniol et al.: Intrinsic and Feedback Dynamics of a Fluidized Bed

Numerical study of the intrinsic and feedback dynamics of a gas-solid fluidized bed

F. Bonniol, C. Sierra, H. Bournot, R. Occelli, L. Tadrif
Laboratoire de l'IUSTI, Polytech' Marseille – DME
5, rue Enrico Fermi, 13453 Marseille Cedex 13

ABSTRACT

The aim of this paper is to understand the complex spatio-temporal patterning of the dense bed when the inlet conditions can be modified by the bed itself. In this study, the inlet conditions (fluid pressure and velocity upstream the bed) take into account resistive effects from the distributor and capacitive ones from the air-supply system (plenum). The present work addresses particularly the issue of the transition between multiple and single bubble regimes that occurs for some particular inlet conditions.

INTRODUCTION

Nowadays the industrial fluidized bed reactors have low pressure-drop air distributor to reduce the cost of blower power: consequently the air supply system (especially the plenum) has an important relation with the movements of the bed. The influence of boundary conditions is a rather new issue in the literature where most of the time numerical simulations assume that the superficial velocity is constant. However it has been shown that this assumption is not always relevant. In *Johnsson et al.* (1) the pressure drop across the air distributor modifies the bed dynamics and in *Kage et al.* (2), *Borodulya et al.* (3), *Baird and Klein* (4) the volume of the plenum appears important also. The variations of these two parameters can induce two particular kinds of behaviour described in *Johnsson et al.* (1): the single bubble regime and the multiple bubbles regime. When the pressure drop of the air distributor is low enough the bed is in the single bubble regime characterized by the eruption of a unique large bubble at a very definite frequency. In this case the pressure fluctuations are directly transmitted to the plenum without attenuation: this is the “coupled case”. On the other hand, for very high pressure drop distributors the bed is in the multiple bubbles regime characterized by a large-band fluctuation spectrum and no interaction with the plenum (“uncoupled case”). To describe these behaviors, the numerical simulation can play an important role. The Eulerian approach to describe both the particles and the gas phase is the most developed (*Peirano et al.* (5), *Sasic et al.* (6)) but with the increase of computational capacity, Eulerian-Lagrangian simulations (*Helland et al.* (7), *Hoomans et al.* (8)) gain interest because of their ability to describe micro-scale mechanism.

NUMERICAL MODEL

The 12th International Conference on Fluidization - New Horizons in Fluidization Engineering, Art. 79 [2007]

It is based on the work of *Helland et al. (7)*. In the simulations, the Eulerian-Lagrangian approach computes the Navier-Stokes equations for the gas phase (we used finite volume resolution with the SIMPLE algorithm) and the Newtonian equations of motion for the particles. For the gas phase we only look at the mass and momentum equation of conservation:

$$\begin{cases} \frac{\partial (\varepsilon \rho_g)}{\partial t} + \nabla \cdot (\varepsilon \rho_g \vec{u}) = 0 \\ \frac{\partial (\varepsilon \rho_g \vec{u})}{\partial t} + \nabla \cdot (\varepsilon \rho_g \vec{u} \vec{u}) = -\varepsilon \nabla \cdot (p \vec{I}) + \mu_g (\nabla \cdot \varepsilon \vec{\tau}_g) + \varepsilon \rho_g \vec{g} - \sum_{i=1}^{N_p(V)} \vec{f}_{drag,i} \end{cases}$$

For the solid phase, for each individual particle, an equation of motion is solved:

$$m_i \frac{d\vec{v}_i}{dt} = m_i \vec{g} + \vec{F}_{drag}$$

The first term is due to gravity and the second to drag between the gas and solid phases. The pressure gradient force, the buoyancy force and the unsteady force have been neglected due to the high solids to gas density ratio. The slip/rotation or Magnus lift force and the slip/shear or Saffman lift force have also been neglected due to the small particle diameter. The drag force follows the equation:

$$\vec{F}_{drag} = \frac{C_d}{8} \pi d_p^2 \rho_g |\vec{u} - \vec{v}_i| (\vec{u} - \vec{v}_i) \varepsilon^2 f(\varepsilon)$$

The drag coefficient C_d on a single sphere is given by *Schiller and Naumann (8)*:

$$\begin{cases} C_d = \frac{24 (1 + 0.15 \text{Re}_p^{0.687})}{\text{Re}_p}, & \text{Re}_p < 1000 \\ C_d = 0.44, & \text{Re}_p \geq 1000 \end{cases}$$

$f(\varepsilon)$ (*Helland et al. (7)*) is a porosity function that take into account the presence of other particles on the drag force. The collisional model used in the simulations is the one proposed by *Walton (10)* based on three constant coefficients.

Fluid inlet boundary conditions

The interaction between the bed and the boundary conditions explained in *Sierra (11)* is characterized by a coupling relation, in which each device (plenum and distributor) acts in a different way. The distributor is a singularity that creates a pressure drop; its effect is characterized by a dissipation coefficient $\bar{\xi}_d$ that depends of the geometry of the distributor and the Reynolds number: $\Delta P_d = (1/2) \rho_g \bar{\xi}_d u_d^2$.

The plenum is a simple cavity usually used to favour a uniform injection of the flow, that acts as a compressible volume in response to the variation of pressure at the bottom of the bed. In this model, each parameter (pressure at the bottom of the bed, in the plenum and inlet velocity) is split into a stationary and a fluctuating part:

$$\begin{cases} p_{p,b}(t) = \bar{p}_{p,b} + \tilde{p}_{p,b}(t) \\ u_d(t) = \bar{u}_d + \tilde{u}_d(t) \end{cases}$$

From continuity of the pressure field along the system and the fluid mass conservation, the pressure coupling between the bed and the plenum is given by a first order differential equation:

$$\frac{d\tilde{p}_p}{dt} + \frac{C_p}{\bar{\xi}_p \bar{p}_p} \tilde{p}_p = \frac{C_p}{\bar{\xi}_p \bar{p}_b} \tilde{p}_b \quad \text{with } C_p = \frac{\gamma \bar{p}_p \Sigma}{\Omega}$$

This equation shows how the plenum reacts (via the distributor) to a variation of pressure imposed to the bed: $\tilde{p}_b(t)$. This form is equivalent to a low-pass filter with $\omega_c = C_p / \rho_g \bar{\xi}_d \bar{u}_d$ the cut-off pulsation. The above equation written for the inlet velocity gives:

$$\frac{d\tilde{u}_d}{dt} + \omega_c \tilde{u}_d = \frac{-1}{\rho_g \bar{\xi}_d \bar{u}_d} \frac{d\tilde{p}_b}{dt}$$

This is the relation we compute for the inlet boundary condition of the flow. When we look at this equation, we see that when $\Omega \rightarrow 0$, $\omega_c \rightarrow \infty$ and as $|d\tilde{p}_b / dt|$ is finite so $\tilde{u}_d \rightarrow 0$: the flow velocity is imposed. And when Ω is large, ω_c diminishes: the plenum cannot follow the dynamics the bed tries to impose because of its natural frequency. Between these two situations, there is a zone where the boundary conditions have a large influence on the dynamics of the bed: there is a volume of the plenum where the coupling is the most important (see e.g. *Baird and Klein (4)*).

Data of the simulation

For the computation the parameters are summarized in *table 1*.

Table 1: Operating conditions used in simulation

Inlet superficial gas velocity	0.2 m/s
Particle diameter	300 μm
Density	3000 kg/m ³
Laminar gas viscosity	1.8x10 ⁻⁵ kg/m/s
Minimum fluidization velocity	0.1 m/s
Fluid time step	10 ⁻⁵ s
Number of particles	200
Riser height x width	0.03x0.003 m
Number of computational cells for the gas flow (Nx x Ny)	16x45

The simulations are done for the coupled case with $\xi_d = 350$ and $\Sigma / \Omega = 0.2$. For the uncoupled case the inlet velocity is imposed at the bottom of the bed.

Initial and boundary conditions:

- Simulations are two dimensional.
- Each simulation starts with the particles randomly dispersed in the computational domain with a nil slip velocity.
- On the lateral faces symmetrical conditions are used for both gas and particles.
- The air inlet is modelled as one dimensional uniform flow.
- The outlet is located at the top of the riser where an outflow condition is used for the gas phase.

Simulation difficulties

During the development of the simulations there were many problems. The simulation of a time variable fluid inlet condition implies precautions because the

system is more unstable from the numerical point of view. For each time step we use a sub-loop to achieve both convergence of the inlet fluid velocity and particle position and velocity. Any sudden change of the inlet flow-rate is taken into account smoothly using an iterative relaxation scheme. If these particular precautions are not observed the drag force calculation over the particles strongly diverges and the calculus stops. We also took particular cautions for the choice of the time step: it has to be small enough to solve the particle dynamics but not too much to insure the convergence of the gas flow calculation.

RESULTS AND DISCUSSION

Figure 1 shows that, in the coupled case the bed is at first in a compact configuration, a bubble appears and goes through the bed until the bed come back to the compact configuration and then a new cycle begins. On the other hand, in the uncoupled case, the bed never reaches such a compact state and many bubbles are present in the bed at the same time.

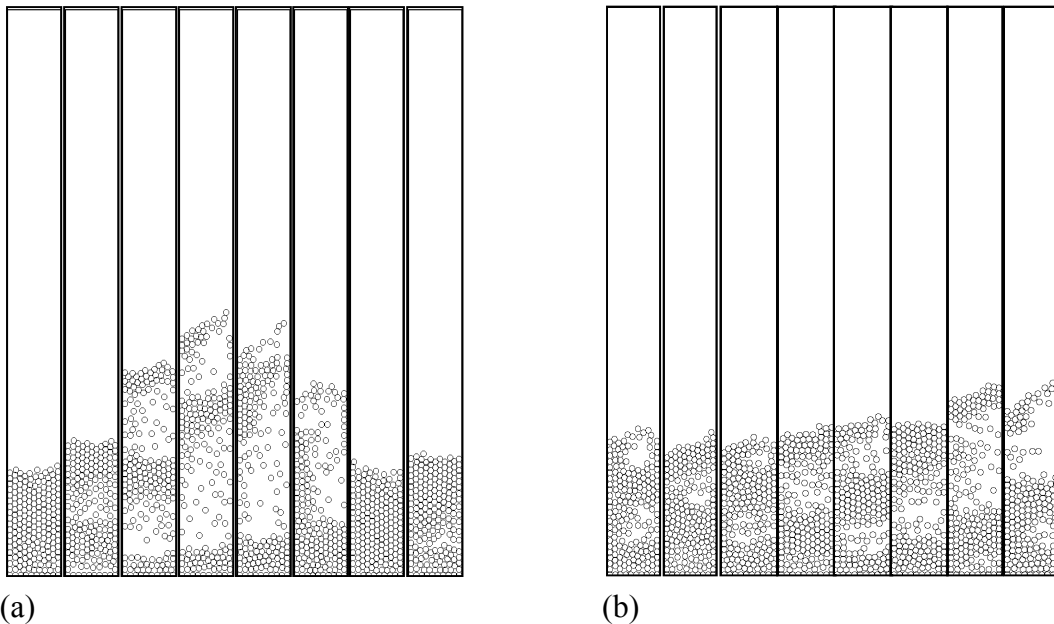


Figure 1: Image sequence of particle positions in the column in the coupled (a) and uncoupled (b) case ($2,1 \times 10^{-2}$ s between frames)

Time and frequency domain analysis

The pressure and velocity signals at the bottom of the bed can be used to characterize fluidization. For the simulation we impose the outlet pressure above the bed (atmospheric pressure) and we calculate the pressure at the bottom of the bed. The results of the numerical simulation are evaluated over a period of 8s. The signal of pressure with and without coupling is shown in figure 2. The corresponding spectra are shown in figure 3.

In the uncoupled case (high pressure drop), there is a generation of small bubbles distributed in the bed and the FFT shows that the signal is characterized by a broad band spectrum around the principal frequency of the bed (the dominant frequency with the maximum amplitude) is around 12 Hz and is close to the theoretical

frequency given by *Baskakov* (12) and $f_b = (g/H_b)^{1/2} / \pi = 12,8$. This regime is similar to the observations made by *Svensson et al.* (1). In the coupled case (low pressure drop and a matched resonant volume of the plenum) the main frequency is smaller (7.5 Hz), the amplitude of the fluctuations is larger and the width of the spectrum diminishes: the bed generates large bubbles that emerge in a very regular way: this is the single bubble regime. The bubble eruption frequency is not controlled anymore by the bed intrinsic dynamics: the bed interacts with the distributor and the plenum and consequently modifies its behavior characterized by a lower frequency. This frequency matches fairly well the simple mass-spring model from *Davidson* (13) given by $f_d = (\gamma \overline{P}_p \Sigma / \rho_s \phi_{cp} h_{cp} \Omega)^{1/2} / 2\pi = 8.1$ Hz. The same kinds of results were found in the experiments of *Svensson et al.* (1) and *Kage et al.* (2). The pressure signal amplitude also increases. Because of the interaction of the bed and the plenum there is a modification of the inlet velocity of the fluid which is not constant anymore (at 0.2 m/s in this case): the bed totally controls the fluid flow and induces such volumic flow rate variations that the velocity can drop down to the minimum fluidization during an oscillation cycle (cf. figure 4).

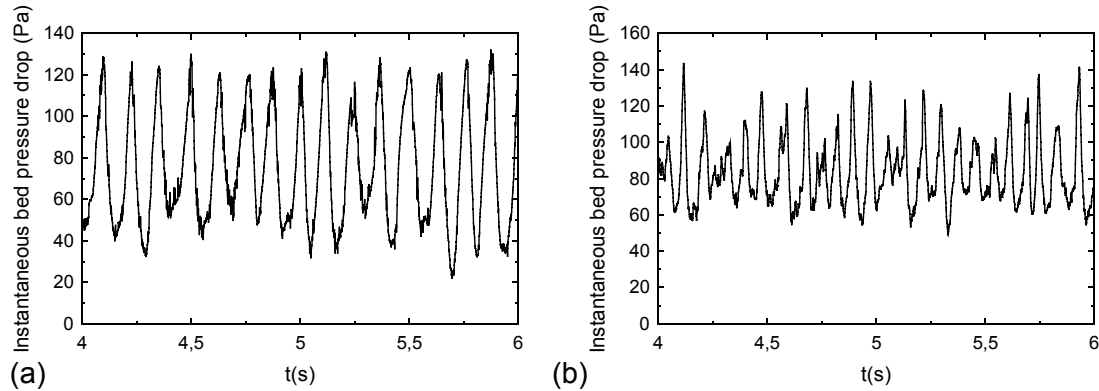


Figure 2: Instantaneous bed pressure drop fluctuations in the coupled (a) and uncoupled (b) case

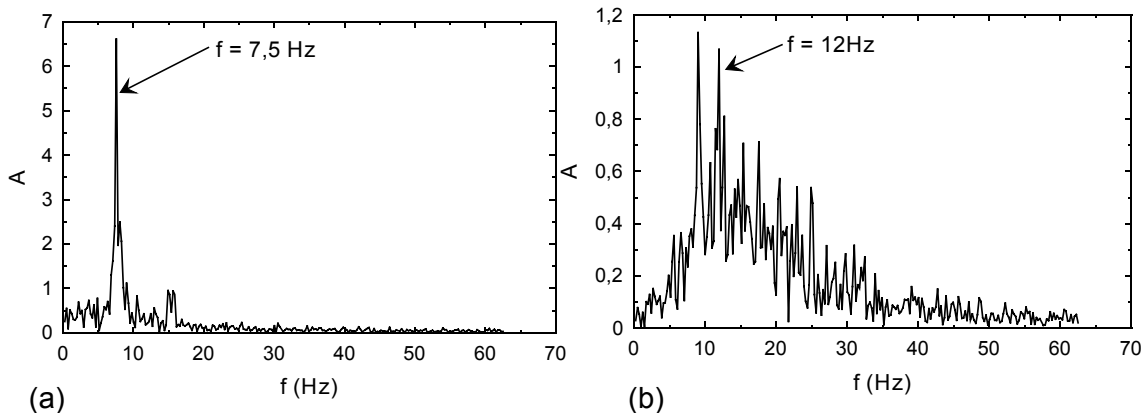


Figure 3: Fast Fourier Transform (FFT) of the pressure signal in the coupled (a) and uncoupled (b) case

The 12th International Conference on Fluidization - New Horizons in Fluidization Engineering, Art. 79 [2007]

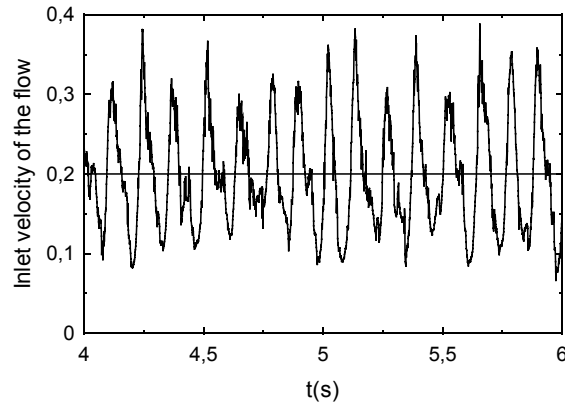


Figure 4: Variations of the inlet velocity of the flow at the bottom of the bed in the coupled and uncoupled case

Spatial analysis

To further illustrate the mutual feedback between the fluid flow and the grain dynamics, figure 5 shows the variations of the bed height for both coupled and uncoupled cases. As expected for the coupled case the motion of the free surface shows a much more regular and large amplitude dynamics.

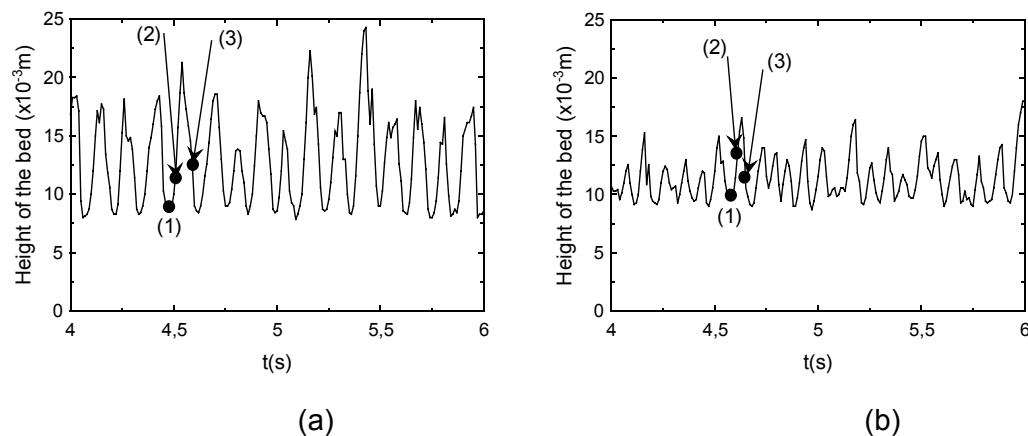


Figure 5: Variations of the bed height in the coupled (a) and uncoupled (b) case

Together with figure 4, we see that the minimum inlet velocity is in phase with the bed height. The drop down of the inlet velocity under the minimum fluidization velocity enhances the recompaction process thus promoting a violent bubble eruption that projects particles upward up to two times the static bed height. For the uncoupled case the bed height variations are less pronounced due to irregular eruptions of smaller bubbles.

From a micro-scale point of view, the individual motion of the particles is also very different. Figure 6 and 7 show a polar diagram of the orientation of the particles velocity vector for both coupled and uncoupled case. Each point corresponds to the number of particles for which the orientation is the same within a defined angle range (15°) at a given time. Each sub-figure (1), (2) and (3) represents the angular-velocity distribution at three different times of a typical oscillation cycle (identified in figure 5). For the most compacted state, the coupled case (fig. 6-1) shows that all the particles are almost at rest at the same time whereas in the

uncoupled case (fig. 7-1), they never reach such a dense state and some clusters keep a slight random motion¹. During the upward acceleration phase (fig. 6-2) and (fig. 7-2), for the coupled case around 80% of the particles are moving together whereas only 40% are doing so for the uncoupled case. This again characterizes, for the coupled case, the burst of a unique bubble that entrains almost all the particles at the same time. Exactly the same tendency is observed when the particles fall back on the distributor (figs. 6-3 and 7-3).

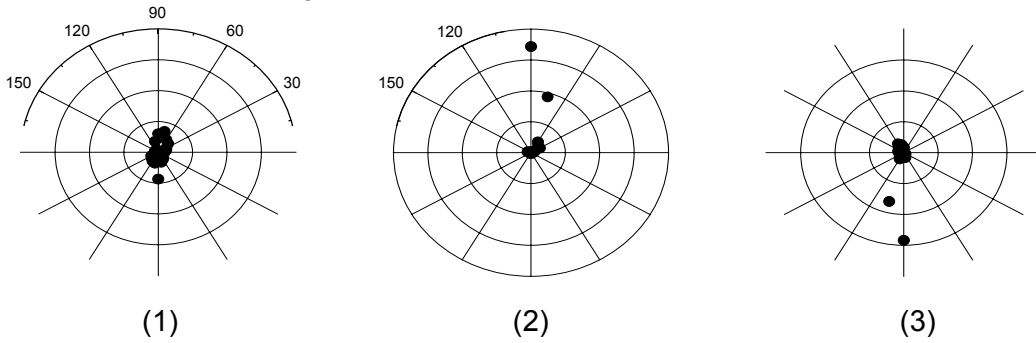


Figure 6: Polar diagram of the velocity of the particles in the coupled case

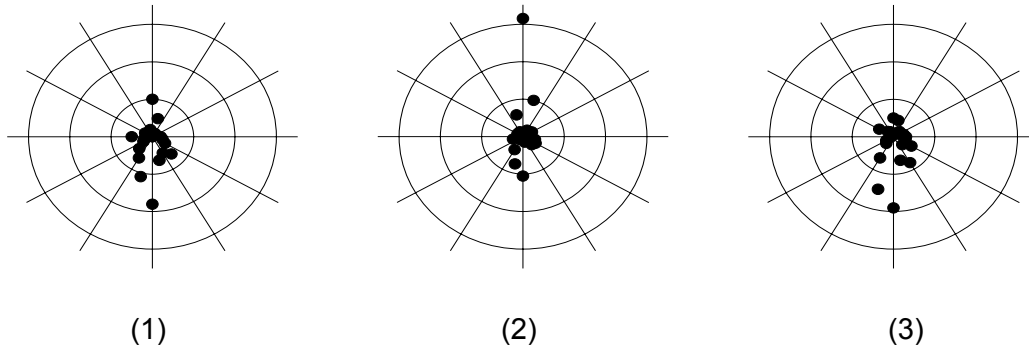


Figure 7: Polar diagram of the velocity of the particles in the uncoupled case

It is important to note that a weak point of these simulations comes from the size of the systems. The confinement interfere with a more detailed comparison of the two regimes. Large scale simulations are clearly required to improve our micro-scale understanding of both regimes.

CONCLUSION

The influence of the fluid inlet conditions has been studied by means of a coupling relation that takes into account the effects of a distributor and a plenum. The numerical Eulerian-Lagrangian simulations were able to reproduce the experimental behaviors on both qualitative and even quantitative grounds (for the temporal dynamics). We were able to identify the multiple and single bubble regimes with their own spatial and temporal characteristics. As a perspective to this work, we plan to use this numerical approach on large scale simulations in order to refine the analysis of the involved local and global scale phenomena. Ongoing work is also currently done to take into account the spatial effect of the distributor for non-uniform fluid inlet profiles.

¹ It is noteworthy that for these two graphs, the velocity orientation is mostly vertical. This is an artefact induced by the lateral confinement of the particles.

SYMBOLS AND ABBREVIATIONS

The 12th International Conference on Fluidization - New Horizons in Fluidization Engineering, Art. 79 [2007]

ΔP_d : pressure drop of the distributor (Pa)	α : gravity acceleration (m^2/s)
ν : adiabatic index (1.4 for air)	ε : porosity (-)
p_n : pressure in the plenum (Pa)	C_d : drag coefficient (-)
ρ_g : gas density (kg/m^3)	\vec{F}_{drag} : drag force (N)
u_d : fluid superficial velocity (m/s)	\vec{f}_{drag} : volumic drag force (N/m^3)
μ_g : laminar gas viscosity ($kg/m/s$)	h_{cp} : close packing bed height (m)
$\bar{\tau}_g$: gas stress tensor (Pa)	N_p : number of particles (-)
d_n : particle diameter (m)	\bar{u} : gas velocity (m/s)
Re_p : particle Reynolds number (-)	\vec{v}_i : particle velocity (m/s)
p_b : pressure at the bottom of the bed (Pa)	ξ_d : pressure drop coefficient of the distributor (-)
Ω : plenum volume (m^3)	Σ : section of the column (m^2)
ρ_s : particle density (kg/m^3)	f_b : frequency given by Baskakov (Hz)
f_d : frequency given by Davidson (Hz)	ϕ_{cp} : close packing compacity (-)

REFERENCES

- (1) A. Svensson, F. Johnsson and B. Leckner, Fluidization regimes in non slugging fluidized beds: the influence of pressure drop across the air distributor, *Powder Technology*, 86 (1996) 299.
- (2) H. Kage, N. Iwasaki, H. Yamaguchi and Y. Matsuno, Frequency analysis of pressure fluctuation in fluidized bed plenum, *Journal of Chemical Engineering of Japan* 24, 1 (1991) 76.
- (3) V. A. Borodulya, V. V. Zav'yalov and Y. A. Buyevich, Fluidized bed self-oscillations, *Chemical Engineering Science*, 40 (1985) 353.
- (4) M. H. I. Baird and A. J. Klein, Spontaneous oscillation of a gas-fluidised bed, *Chemical Engineering Science*, 28 (1973) 1039.
- (5) E. Peirano, V. Delloume, F. Johnsson, B. Leckner and O. Simonin, Numerical simulation of the fluid dynamics of a freely bubbling fluidized bed: influence of the air supply system, *Powder Technology*, 122 (2002) 69.
- (6) S. Sasic, F. Johnsson and B. Leckner, Inlet boundary conditions for the simulation of fluid dynamics in gas-solid fluidized beds, *Chemical Engineering Science*, 61 (2006) 5183.
- (7) E. Helland, R. Occelli and L. Tadriss, Numerical study of cluster formation in a gas-particle circulating fluidized bed, *Powder Technology*, 110 (2000) 210
- (8) B. P. B. Hoomans, J. A. M. Kuipers and W. P. M. Van Swaaij, Granular dynamics simulation of cluster formation in dense riser flow, 3rd Int. Conf. on Multiphase Flow, (1998).
- (9) L. Schiller and A. Z. Naumann, A drag coefficient correlation, *Ver. Deut. Ing.*, 32 (1954) 35.
- (10) O. R. Walton, Quarterly report Jan-Mar 1988, Lawrence Livermore Nat. Lab.
- (11) C. Sierra and L. Tadriss, About frequency coupling between riser and plenum in a gas fluidized bed, *Comptes Rendus de l'Academie des Sciences Series IIB Mechanics Physics Astronomy*, 328 (2000) 323.
- (12) A. P. Baskakov, V.G. Tuonokov and N. F. Fillippovsky, A study of pressure of pressure fluctuation in a bubbling fluidized bed, *Powder Technology*, 45 (1986) 113.
- (13) J. F. Davidson, *Inst. Chem. Eng. Symp. Sr.*, 30 (1968) 3.